Hardening mechanisms of ionic crystals on {110} and {100} slip planes

— **Source link**

Werner Skrotzki, Peter Haasen

Institutions: University of Göttingen

Topics: Slip (materials science), Critical resolved shear stress, Hardening (metallurgy) and Anisotropy

Related papers:

- Temperature and rate dependent deformation of halite

- Theory of Dislocations

- Rheology of rocksalt

- Dislocations and the plasticity of ionic crystals

- Solution hardening by aliovalent cations in ionic crystals

HARDENING MECHANISMS OF IONIC CRYSTALS ON 110 AND 100 SLIP PLANES

W. Skrotzki, P. Haasen

HARDENING MECHANISMS OF IONIC CRYSTALS ON {110} AND {100} SLIP PLANES

W. Skrotzki and P. Haasen

Institut für Metallphysik, Universität, Göttingen, RFA.

Résumé.- Les cristaux ioniques de la structure NaCl peuvent être déformés sur plusieurs plans cristallographiquement non-équivalents. La résistance à la déformation varie avec le type du système de glissement. Cette anisotropie plastique dépend de la température, du dopage bivalent et de l'ionicité du matériau. C'est démontré par des mesures de la limite élastique pour le glissement sur les plans{110} et {100}. Pour une série de cristaux du type NaCl les mécanismes de durcissement qui sont basés sur les interactions de Peierls et dislocation-solute sont discutés. L'anisotropie plastique est une aide substantielle pour l'analyse de ces interactions.

Abstract.- Ionic crystals of the NaCl structure can be deformed on several non-equivalent crystallographic planes. The hardness varies with the type of slip system. This plastic anisotropy depends on temperature, divalent doping and ionicity of the material as is shown by measurements of the critical resolved shear stress for slip on {110} and {100} planes. For a series of NaCl-type crystals hardening mechanisms are discussed based on Peierls and dislocation-solute interactions. The plastic anisotropy is of substantial help in the analysis of these interactions.

1. Introduction.- The hardening of ionic crystals has been frequently investigated. Nevertheless, the interaction mechanisms determining the critical resolved shear stress (CRSS) of these materials are still under dispute. Suzuki and Kim /1,2/ in agreement with calculations of Granzer et al. /3/ conclude from their measurements of the CRSS of relatively pure crystals, that at low temperatures the overcoming of the Peierls potential is responsible for the CRSS. Frank /4/ as well as Suszynska /5/ and Grau and Fröhlich /6/ assume that in doped crystals at medium temperatures the elastic interaction of screw dislocations with divalent ion vacancy dipoles or aggregates of such dipoles determines yielding. These investigations are, however, limited to {110}<110> glide. {100}<110> slip could be realized as well in previous work /7/. It showed that for the understanding of the plastic anisotropy electrostatic interactions have to be taken into account.

 The purpose of the present paper is to present detailed information on slip mechanisms in ionic crystals from extended measurements of the dependence of the CRSS on temperature, divalent doping, slip system and ionicity of several materials. Especially the plastic anisotropy helps to decide whether models based on elastic or electrostatic inter-

actions are able to describe the onset of the plastic deformation.

2. Experimental.- The experiments were carried out on alkali and silver
halide single crystals grown by the Kyropoulos method. For the growth
of silver chloride crystals NaCl seed crystals were used /8/. Starting
material, dopants and growth parameters are listed in table I.

Table I.- Crystal growth parameters

	Starting material (origin)	Atmosphere	Crucible	Dopant
NaCl	suprapur (Merck, FRG)	Air	Porcelain	$SrCl_2$
KCl	pro analysi (Merck)	Air	Porcelain	$SrCl_2$
KBr	pro analysi (Riedel de Häen,FRG)	Air	Porcelain	$SrBr_2$
KJ	suprapur (Merck)	Argon	Platinum	SrJ_2
AgCl	optipur (Merck)	Argon	Quartz	$CaCl_2$

Purity was determined by atomic absorption analysis. <100>- orientated
specimens with {100}-side faces could be obtained by cleavage, while
<111>-or <557> -orientated specimens with {110}- and {112}- or {110}-
and {7,7,10}- side faces, respectively, had to be string sawn with water.
In the case of the AgCl crystal all specimens had to be sawn using a
fixing reagent in dark room red light. The orientation of the AgCl sam-
ples could be easily found with the aid of the <100>-orientated NaCl
seed crystal. The accuracy amounted to 3 degrees. Specimen dimensions
were about 4x4x18 mm³. Before testing all samples were annealed on a
platinum foil for 20 h at ∿0.85 T_m (T_m = melting temperature). Annealing
and growth atmosphere were identical. The standard cooling rate was
about 1 K/min. (SC), while for some specimens quenched from 700 K it
was about hundred times higher (Q). All samples have been polished first
mechanically on wetted silk and then chemically in different solutions.
Suitable etchants to reveal dislocations were found. Details of the po-
lishing and etching procedures are given in /9/.

The deformation was performed in dynamic compression using an In-
stron-machine. The average strain rate was about $\dot{\epsilon} \approx 10^{-4} s^{-1}$. Room tem-
perature deformation was performed in air. For lower and higher tempe-
ratures suitable compression devices were immersed in baths of liquid
helium, liquid nitrogen, isopentane and silicon oil. The AgCl crystals
were deformed in darkroom red light.

3. Results.- 3.1 Slip_on_{100}_planes_produced_by_compression.- In ionic
crystals single slip on {110} or {100} planes has previously been achie-
ved in shear tests /7/. This deformation method has however the disad-
vantage that it can be used only at room temperature (RT). Therefore we
have realized it by compression of suitably orientated crystals. In this
section it will be shown that large scale macroscopic slip on {100} pla-
nes alone could be realized over a wide range of temperature.

Assuming Schmid's law in crystals of any orientation a slip sys-
tem with the CRSS τ_c will be activated first if the condition $\tau_c < \tau_{ci} \cdot S_1/S_i$ is fullfilled (S_1 = Schmid factor of the first system, S_i, τ_{ci}
those of the other systems). Thus slip on a {110} or a {100} plane alo-
ne is to be expected only for orientations adjacent to <100> and <111>,
respectively.

Deforming crystals in <100>-orientation ($S_{max}(\{110\}<110>) = 0.5$,
$S_{max}(\{100\}<110>) = 0$) slip usually starts on more than one {110}<110>
system (Fig. 1).

KCl

[001]   [5$\bar{5}$7]

(100)   (010)   (110)   ($\bar{7}$710)
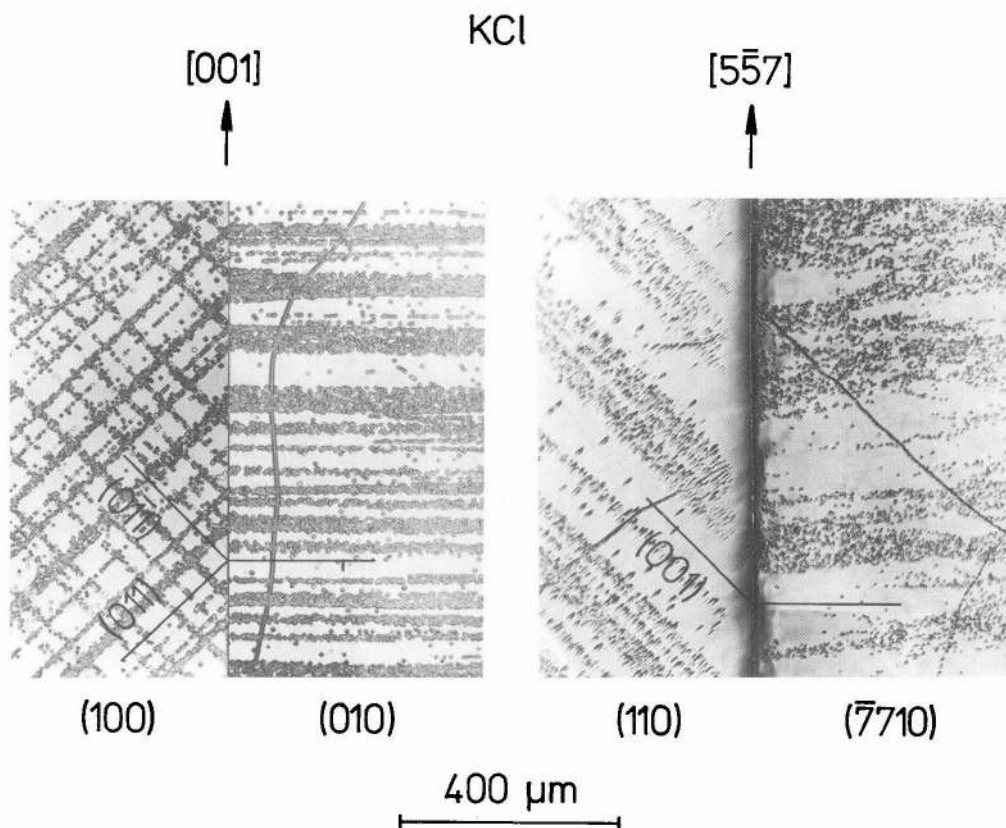
400 μm

Fig. 1.- Etched surfaces of square KCl crystals ($c_{Sr^{2+}}$ = 56 ppm) deformed along [001]
and [5$\bar{5}$7] in compression at RT.

Using <557> ($\cong$ <111> +10°) -orientated crystals ($S_{max}(\{110\}<110>)$ = 0.12, $S_{max}(\{100\}<110>)$ = 0.5) deformation begins on a single {100} plane (Fig. 1). Particularly interesting is the difference in the slip bands produced by the screw dislocations (Fig. 1 : side faces (010) and (7,7,10)). Changing to the <111> -orientation ($S_{max}(\{110\}<110>)$ = 0, $S_{max}(\{100\}<110>)$ = 0.47) three {100}<110> systems are equally stressed. Hence, slip on more than one {100} plane has been observed (Fig. 2). This is demonstrated by the etch pit traces on the $(\bar{1}12)$ side face as well as on the (001) cleavage plane. The absence of traces on the (001) plane perpendicular to $[1\bar{1}0]$ means that traces on $(\bar{1}12)$ perpendicular to $[1\bar{1}1]$ are produced by screw dislocations which have moved on (001). It is emphasized that for all the investigated crystals {111}<110> slip has never been observed, contrary to the statements of Bhagavan Raju and Strunk /10/.
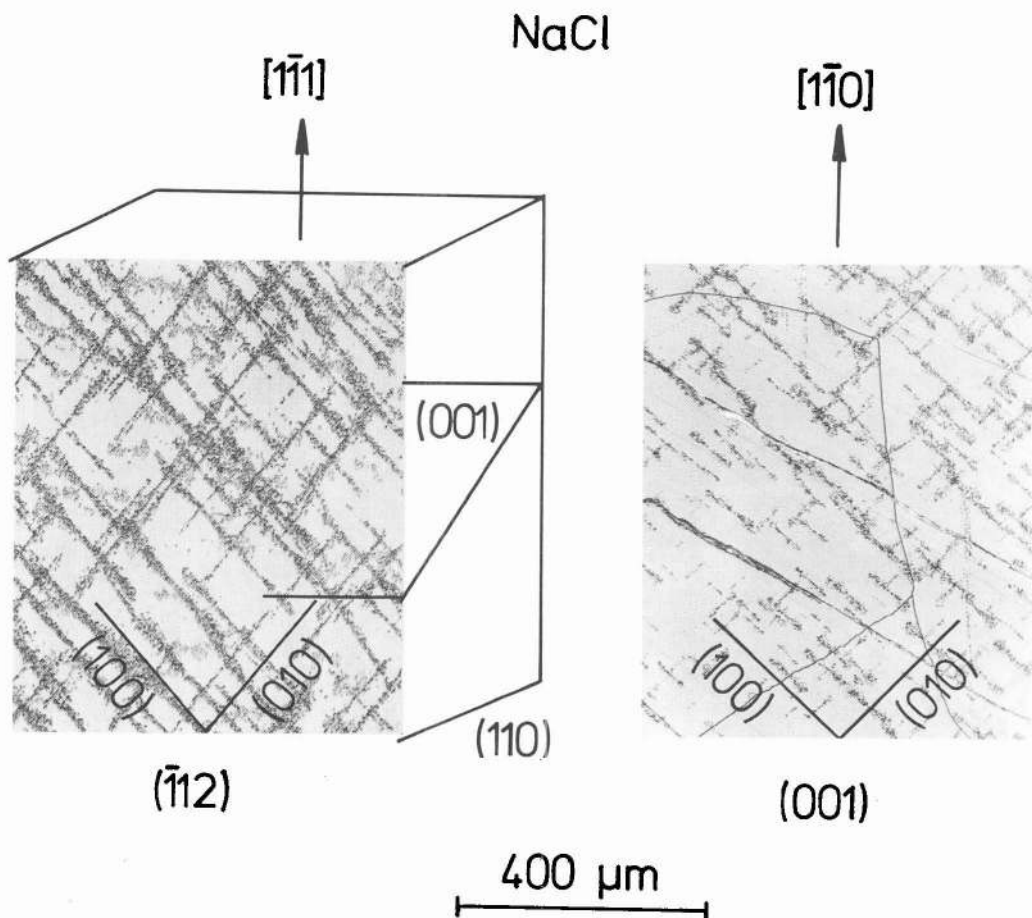

Fig. 2.- Etch pit arrangement on the $(\bar{1}12)$ side face and the (001) cleavage plane of NaCl (c_{Sr2+} = 63 ppm) after RT deformation of <111> -orientated crystals.

Because of multiple slip the <111> -orientated crystals show strong work-hardening which decreases with increasing doping (Fig.3).

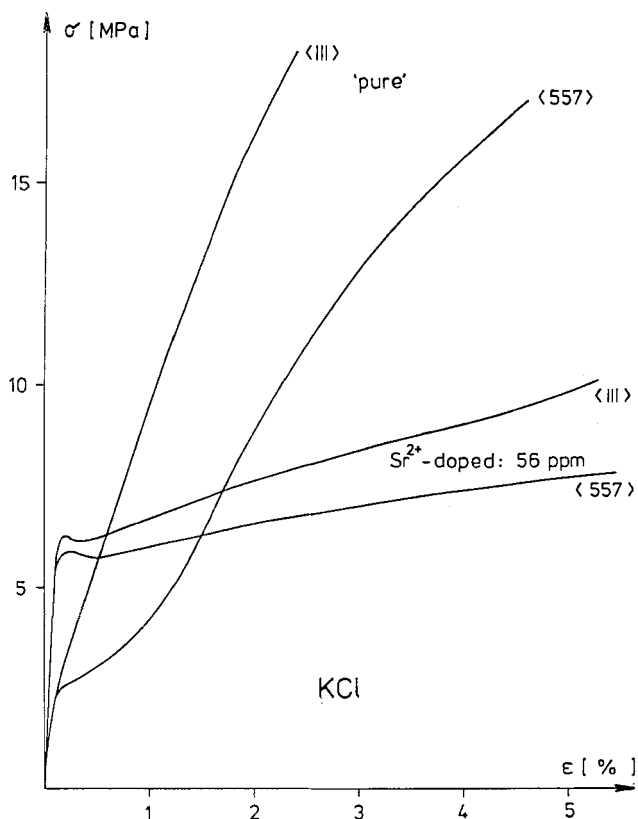Fig. 3.- RT stress-strain curves of "pure" and Sr^{2+} doped KCl crystals compressed in <111> and <557> orientations.

Therefore <557>-orientated crystals are preferred for the determination of the CRSS on {100}. However, this is only possible as long as the ratio $\tau_c^{\{100\}}/\tau_c^{\{110\}}$ is smaller than that of the Schmid factors ($S^{\{100\}}/S^{\{110\}} = 4$).

The movement of edge and screw dislocations in dependence of temperature, doping, slip sytem and ionicity of the material will be described in a separate paper.

3.2. Measurements of the CRSS.- 3.2.1. Determination of the CRSS.- In ionic crystals the onset of the plastic deformation marks itself in different ways in stress strain curves (SSC). A schematical description of typical SSC and of the determination of the CRSS from them is given in figure 4.
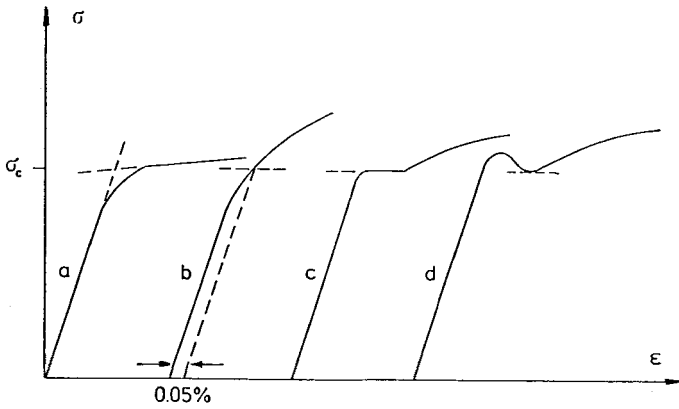
Fig. 4.- Typical initial stages of stress-strain curves and determination of the CRSS.

Most specimens showed SSC of type a). Curves of type b) have been observed for <111>-orientated crystals. Parabolic curves were shown by all orientations at high temperatures, for <557>- and <111>-orientations also at low temperatures. Curves of type c) and d) have only been observed for doped crystals. The maximum scatter of the CRSS of identical specimens was 5 %.

3.2.2 Dependence of the CRSS on temperature and doping.- In ionic crystals a decrease of the CRSS with increasing temperature occurs in several regimes, schematically presented in figure 5. Crystals doped with a certain concentration of divalent impurities show a decrease in four regimes. With increasing purity of the material the temperature dependence of the CRSS approaches that indicated by the dotted line.
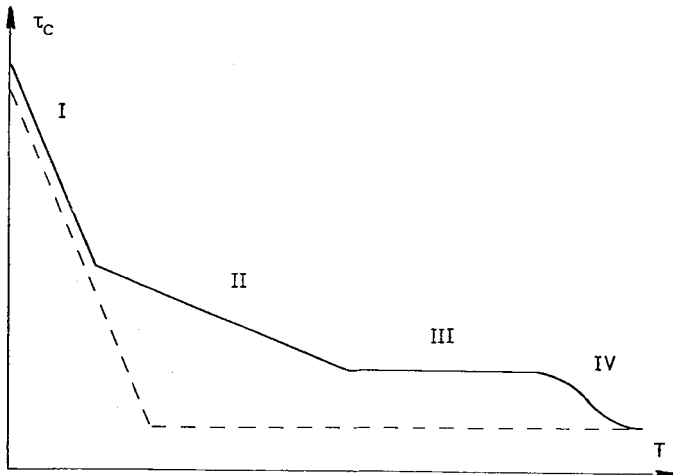

Fig. 5.- Schematic regimes of the temperature dependence of the CRSS of ionic crystals. Dotted and traced lines belong to "pure" and doped crystals, respectively.

In the following these regimes will be characterized in terms of
the dependence of the CRSS on temperature, doping, slip system and io-
nicity of the material.

Regime I.- Details on regime I for {100} slip have been presented else-
where /11/. Here further results will be presented which demonstrate
the intrinsic plastic anisotropy. Figure 6a shows the temperature depen-
dence of the CRSS for slip on {110} and {100} planes. The values for
$\tau_c^{\{100\}}$ marked by half-filled symbols have been obtained by extrapola-
tion from KCl-KBr solid solutions /11/. Striking is the strong plastic
anisotropy below a certain temperature which depends on the material.
The usual scaling of different materials in terms of the shear modulus
and the melting temperature does not work for ionic crystals (Fig. 6b).
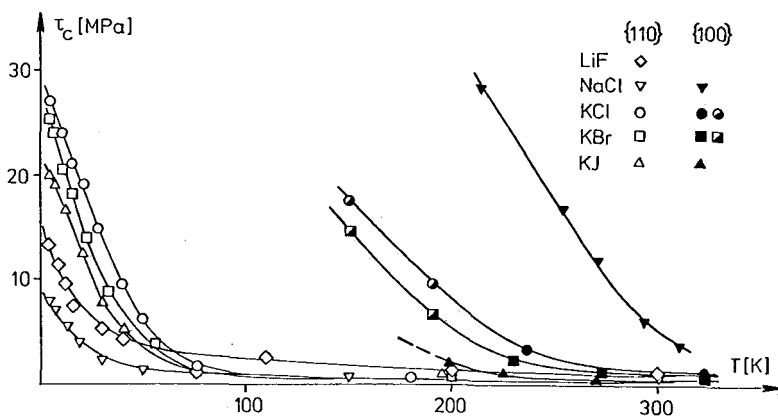
Fig. 6a.- Temperature dependence of the CRSS of "pure" crystals. Half-filled symbols
are extrapolated from KCl-KBr solid solutions (◇/1/, ▽/2/, o □ △ by T. Suzuki (to
be published), ▼ /12/)
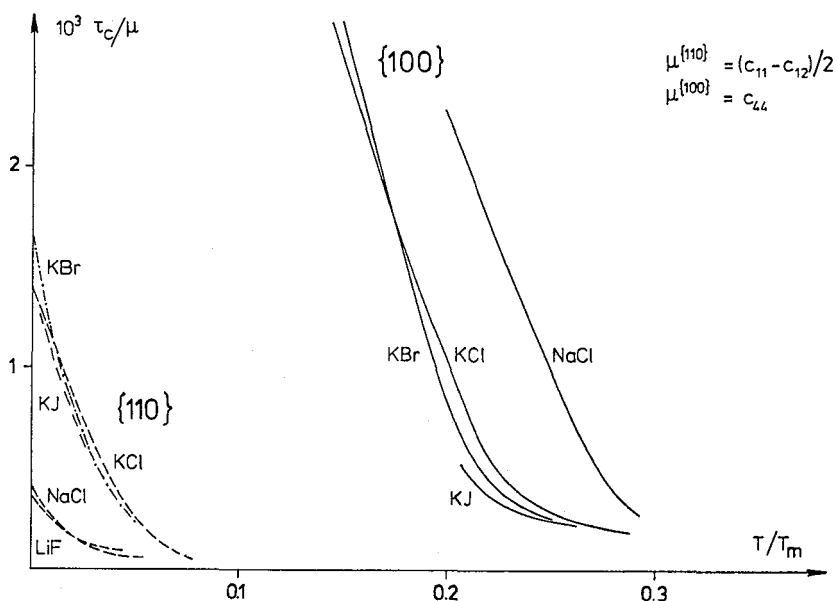
Fig. 6b.- Curves of (a) reduced by the shear modulus μ and the melting temperature T

The dependence of the CRSS on divalent doping is presented in figures 7 and 8.
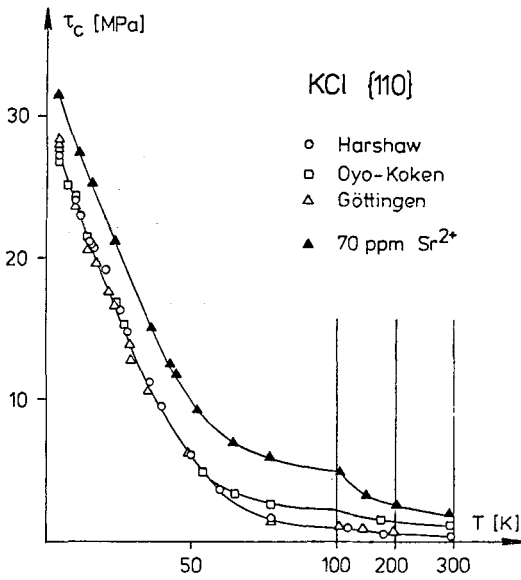
Fig. 7.- Temperature dependence of the CRSS of KCl for {110} slip. Open symbols represent "pure" crystals of different origin.
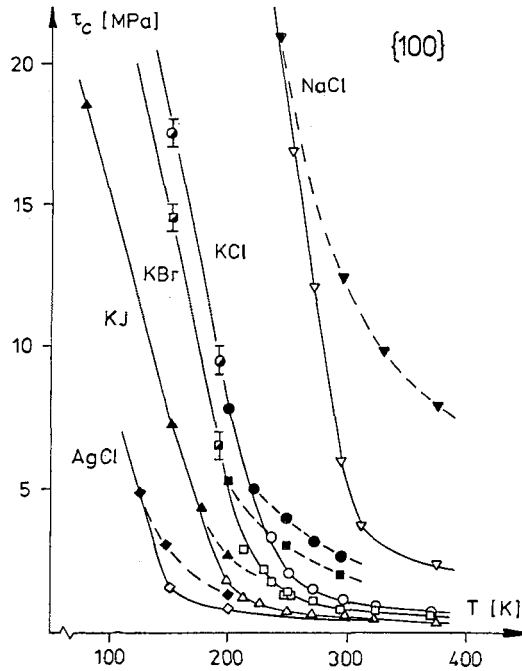
Fig. 8.- Temperature dependence of the CRSS for {100} slip. Open and filled symbols represent pure and divalent doped crystals (▼ 113, ● 56, ■ 94, ▲ 89 ppm Sr^{2+} ; ◆ 483 ppm Ca^{2+}).

Doped crystals show the same temperature dependence in regime I as "pure" ones. Moreover, doping has a greater influence on {110} than on {100} slip. For {100} the CRSS of the doped crystals agree with those of the "pure" ones at low temperatures. Remarkable is also the good agreement between the CRSS of "pure" crystals of different origins (Fig.7). The solution hardening of KCl τ_c (70 ppm Sr^{2+}) relative to τ_c ("pure") for {110} slip amounts to about 10% at 4.2 K. It is also noted that the activation volume is smaller than 100 b^3 in regime I /11/.

Regime II.- In figures 9a-e the temperature dependence of the CRSS is presented in such a way that regimes II-IV can be recognized clearly. A comparison of these figures shows a qualitative similarity between all the materials investigated. The temperature dependence of the CRSS is smaller in regime II than in regime I, see figure 9b. With increasing purity of the material the decrease in τ_c(T) becomes smaller.
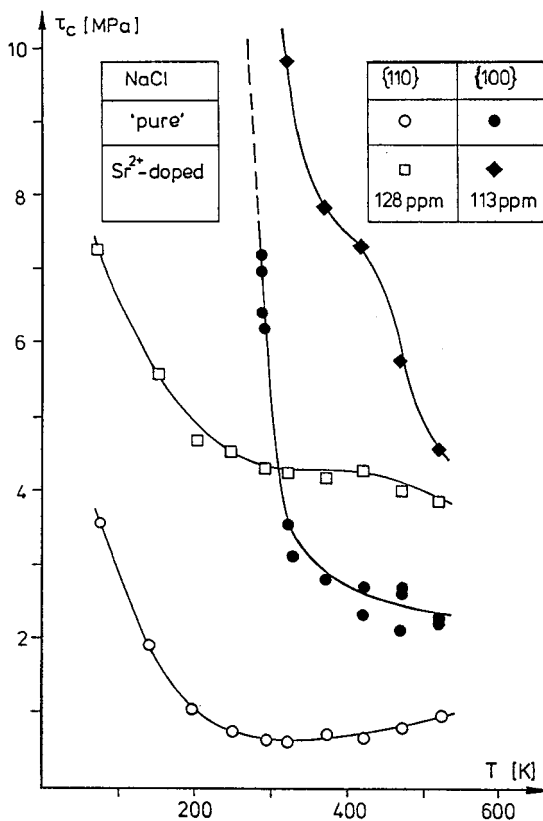
Fig. 9a.
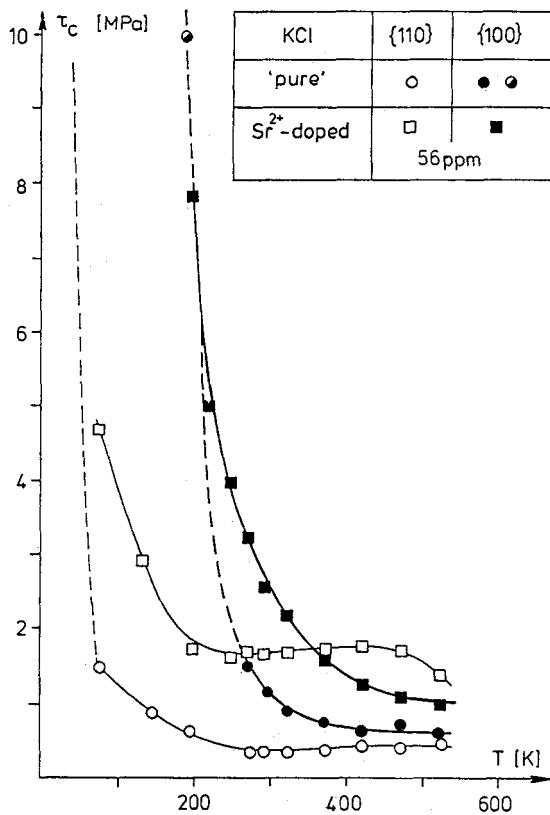
Fig. 9b.
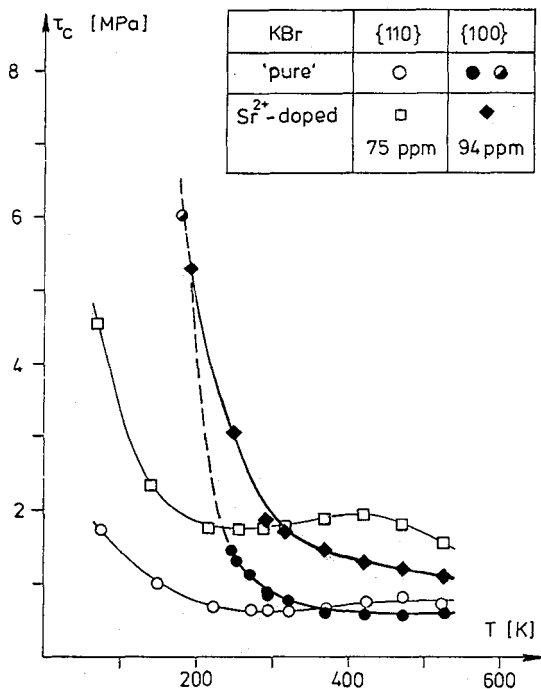
Fig. 9c.
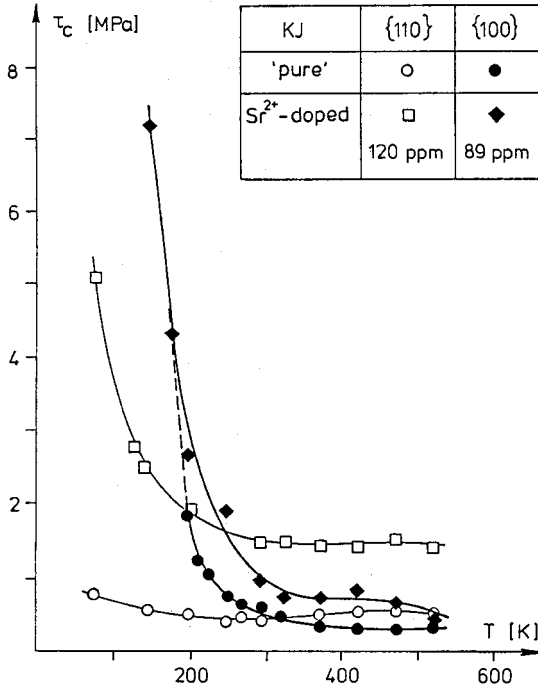
Fig. 9d.
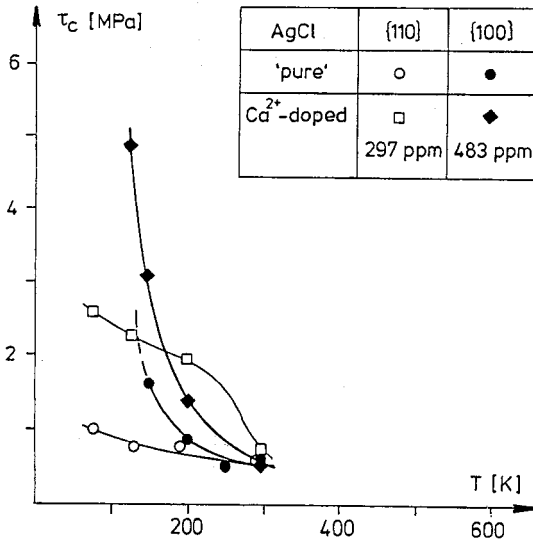
Fig. 9e.

Fig. 9a-e.- Temperature dependence of the CRSS of "pure" and doped crystals for slip on {110} and {100} planes.

The concentration dependence of the CRSS shown in figures 10a and b is more or less parabolic depending on the material. Values for $\tau_c^{\{100\}}$ obtained using crystals of different orientations agree well (Fig. 10b).
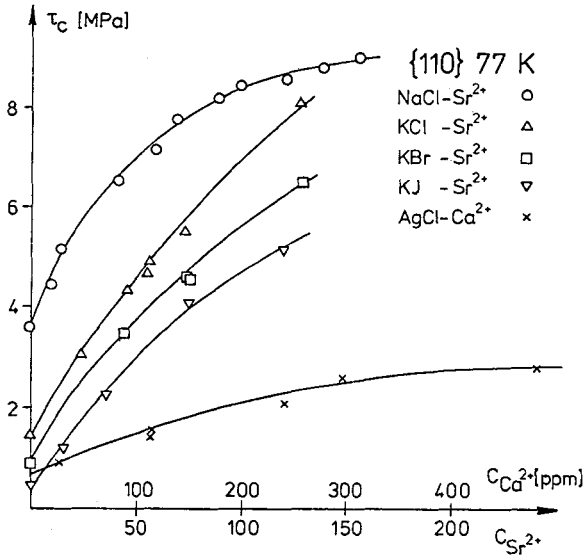
Fig. 10a.
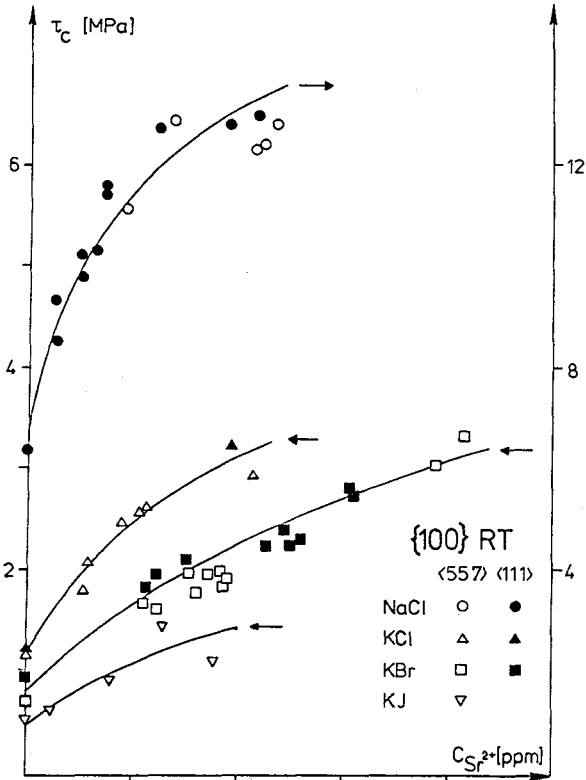
Fig. 10b.

Fig. 10a-b.- Concentration dependence of the CRSS for {110} (a) and {100} slip (b) in regime II

Regime III.- Here the CRSS is nearly temperature independent (Figs. 9 a-e). With increasing temperature sometimes a weak increase is observed. Figures 11a and b show the dependence of the CRSS on divalent doping. For all materials and concentrations investigated (except NaCl-Sr^{2+}) the CRSS is a linear function of the dopant concentration $c_{Me^{2+}}$ (for the alkali halides $c_{Sr^{2+}} \lesssim 150$ ppm, for AgCl $c_{Ca^{2+}} \lesssim 500$ ppm). Quenching experiments on Sr^{2+} doped NaCl, KCl and KBr crystals showed that only the NaCl-Sr^{2+} hardening is strongly dependent on the cooling rate (Fig. 12). The CRSS of quenched NaCl-Sr^{2+} depends also linearly on the dopant concentration. The quenching effect on the slope of $\tau_c(c_{Sr^{2+}})$ for KCl and KBr is only 14 and 4 %, respectively.
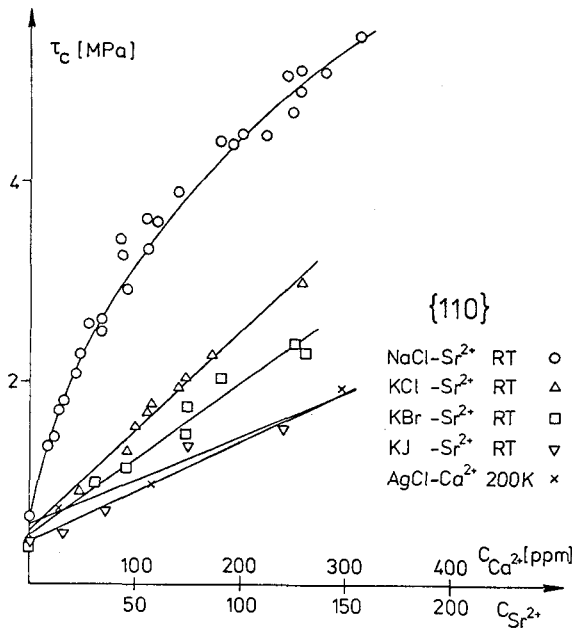
Fig. 11a.
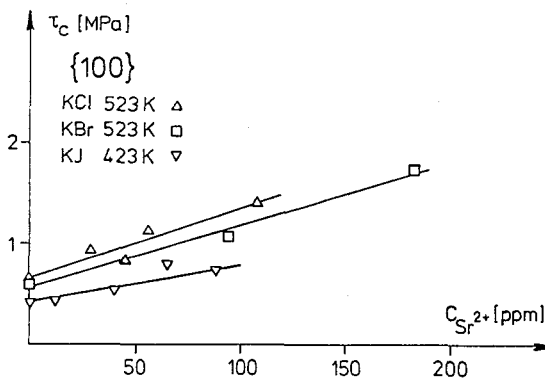
Fig. 11b.

Fig. 11a-b.- As figure 10 for regime III.
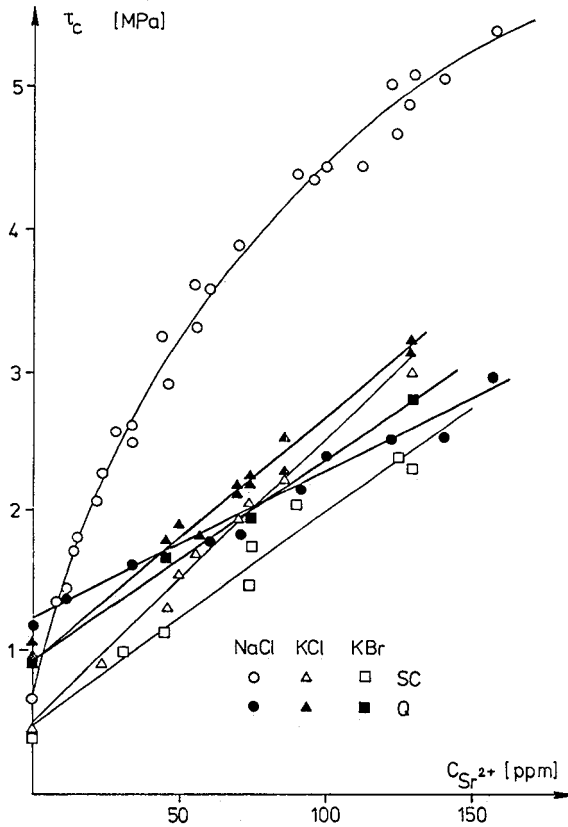
Fig. 12.- Concentration dependence of the CRSS for {110} slip at RT after cooling
with different rates.

We would like to point out that quenching experiments are more
problematic than frequently described. This is already indicated by an
increase of the CRSS of "pure" crystals by a factor of two due to quen-
ching. Parallel to that an increase of the dislocation density from
2×10^4 to 2×10^6 cm^{-2} is observed. So quenching does not only change the
impurity aggregation state but also the dislocation-dislocation inter-
action. Qualitatively the same results have been obtained under compa-
rable conditions by Suszynska /5/ for NaCl-Sr^{2+} while for KCl-Sr^{2+} the-
re exists large discrepancy between her results and ours.

The effect of the cooling rate on the temperature dependence of
the CRSS is shown for NaCl-Sr^{2+} in figure 13. The CRSS of quenched
crystals decreases much more strongly with increasing temperature than
that of slowly cooled samples. Below a certain temperature quench-har-
dening, above quench-softening occurs. Above RT the CRSS for {110} slip
in quenched crystals is increasing with temperature. In the same tempe-

rature range a change in slope for $\tau_c^{\{100\}}$(T) is observed, too. The same behaviour has been described by Johnston/13/ for {110} slip in LiF-Mg^{2+}.
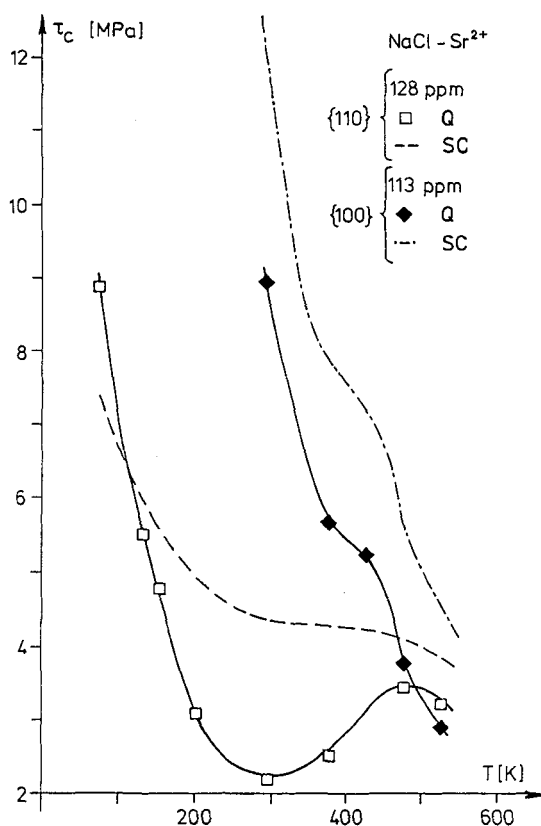
Fig.13.- Temperature dependence of the CRSS of NaCl-Sr^{2+} after different cooling treatments.

Regime IV.- Here the CRSS decreases towards a temperature independent limit. This decrease sets in at $T_f \approx 500$ K for the alkali halides and at $T_f \approx 250$ K for AgCl, reflecting a difference in the melting temperatures of these materials (AH: T_m = (1074-954 K), AgCl: T_m = 728 K). An early high temperature drop shortens regime III, to be seen for {100} and {110} slip in figures 9a and b, respectively.

4. Analysis and discussion of the results.- 4.1 Peierls mechanism (regime I).- The strong temperature dependence of the CRSS as well as the small activation volume suggest the Peierls mechanism as the rate controlling process in regime I. This has already been confirmed for {110} and {100} slip /1,2,11/ by a detailed analysis of the low temperature results. A summary including some results given in section 3.2.2 is presented in table II.

Table II.- Experimental Peierls stresses, sum of the polarizabilities of the matrix ions ($\Sigma\ \alpha$), static dielectric constant (ε_o) and Cauchy relation (c_{12}/c_{44}).

		LiF	NaCl	KCl	KBr	KJ	AgCl
τ_p[MPa]	{100}	(~320)*)	140	80	70	50	~ 35
	{110}	20	11	35	35	28	
$10^3\tau_p^{\{hkl\}}/\mu^{\{hkl\}}$	{100}	(~5)	10	12	14	12	~ 5
	{110}	0.5	0.5	1.6	1.9	1.8	
$\Sigma\alpha$ [10^{-30}m³]		0.90	3.21	4.13	5.25	7.28	4.97
ε_o		8.5	5.45	4.49	4.52	4.68	9.55
c_{12}/c_{44}		0.65	0.84	0.81	1.06	0.6	5.67

*) Estimated from torsion experiments of Gilman /14/.

From this table the following can be ascertained:

- $\tau_p^{\{100\}} > \tau_p^{\{110\}}$, i.e. the intrinsic resistance to glide on {100} is stronger than on {110} planes.

- $(\tau_p/\mu)^{\{100\}} \approx (10-14) \times 10^{-3}$, (LiF $\approx 5 \times 10^{-3}$), AgCl $\approx 5 \times 10^{-3}$; $(\tau_p/\mu)^{\{110\}} \approx (0.5-1.9) \times 10^{-3}$ i.e. the reduced glide resistance is about one order of magnitude larger on {100} than on {110}. The correlation of the Peierls stresses with the shear modulus μ is particularly poor for the alkali halides on {110}.

- $\tau_p^{\{100\}}$ decreases in the series from LiF to AgCl while $\tau_p^{\{110\}}$ does not.

     Since Buerger /15/ the intrinsic resistance to slip on {100} planes has been correlated with the polarizability ($\Sigma\alpha$) of the ions constituting the crystal. With increasing $\Sigma\alpha$ a decrease of $\tau_p^{\{100\}}$ has been expected. The results on AgCl show however, that the polarizability which is directly connected with the static dielectric constant is not the only parameter determining {100} slip. In comparison with the alkali halides the Cauchy relation is strongly violated in AgCl. As pointed out by Bücher /16/ this violation is essentially caused by a large three-body contribution to the Van der Waals interactions. Furthermore the quadrupolar deformability of the silver ion seems to be relevant. Differences between AgCl and the alkali halides have also been attributed to covalent binding in the silver halides. However, neither calculations nor x-ray measurements of the electron density distribution give evidenc for such a contribution /17/.

     The Peierls stress of a crystal has been calculated with elastic and atomistic models. Only the atomistic calculations give reasonable values for τ_p and above all describe the plastic anisotropy correctly

/11/. Calculated values are for NaCl: $\tau_p^{\{100\}}$ = 220 MPa /18/, $\tau_p^{\{110\}}$ = (14.1-21.5) MPa /3/, (17.3/80.0) MPa /19/, for KCl: $\tau_p^{\{110\}}$ = (12.7-32.4) MPa /20/, 30.4 MPa /21,22/. These values should be compared with table II. An extension of these calculations, especially to the silver halides with Van der Waals binding would be of great interest.

Our investigation on the influence of doping on the CRSS in regime I shows that the observed increase seems to be additive to the low temperature steep increase of the CRSS for the "pure" crystals. These results differ from those obtained for alkali halide solid /23/ and bcc metallic alloys, both of which show alloy-softening in a certain temperature range. Further investigations of the doping effect on the Peierls mechanism in ionic crystals are planed.

4.2 Dislocation-solute interaction.- It is inferred from the dielictric loss measurements /24/ that for small concentrations and after a suitable thermal treatment the divalent impurities are paired with vacancies as required for charge compensation in the form of 'impurity-vacancy-dipoles' (IV-dipoles). For our standard cooling rate this condition seems to pertain in all crystals investigated except NaCl-Sr^{2+}. Here quenching experiments show that analogous results can be obtained only by using a cooling rate which is about hundred times higher. The Sr^{2+} doped NaCl crystals pretreated under standard conditions will be discussed separately in section 4.3.

4.2.1 Short-range interaction of dislocations with IV-dipoles (regime II). - The temperature as well as the concentration dependence of the CRSS suggest the onset of plastic deformation in regime II to be determined by a short-range interaction with IV-dipoles. For dilute alloys standard theories of solide solution hardening yield for this contribution /25/:

$$\Delta\tau_c = \frac{f^{3/2}}{(2E_L)^{1/2}\, b}\, c_p^{1/2}\, (1-\phi(T)) \qquad (1)$$

(c_p = doping concentration per unit area of the slip plane, $c_p \sim c$; f = maximum interaction force solute-dislocation; E_L = line tension; the temperature dependence (see eq. (4)) $\phi(T) = 0$ for T = O K). As will be shown in detail in section 4.2.4 from a comparison of the plateau stresses for {100} and {110} slip, even the CRSS of our purest crystals is determined by unknown background impurities. According to computer simulations /26/ of the movement of a dislocation over a statistical distribution of point obstacles of equal strength the CRSS contribution of the "pure" component is eliminated using a quadratic superposition

law: $\Delta\tau_c = (\tau_c^2 - \tau_{cu}^2)^{1/2}$, ($\tau_{cu}$ = CRSS of the "pure" crystals). τ_{cu} includes an athermal part τ_μ, which is assumed to be independent of doping. According to Frank /27/, doped crystals are filled during microstraining with dislocations until their interaction stress matches the CRSS determined by the doping. Figure 14 shows that the $c^{1/2}$ dependence of $\Delta\tau$ is rather well established in regime II.

	{110}	{100}
	77K	RT
KCl	▽	▼
KBr	□	▣
KJ	○	●
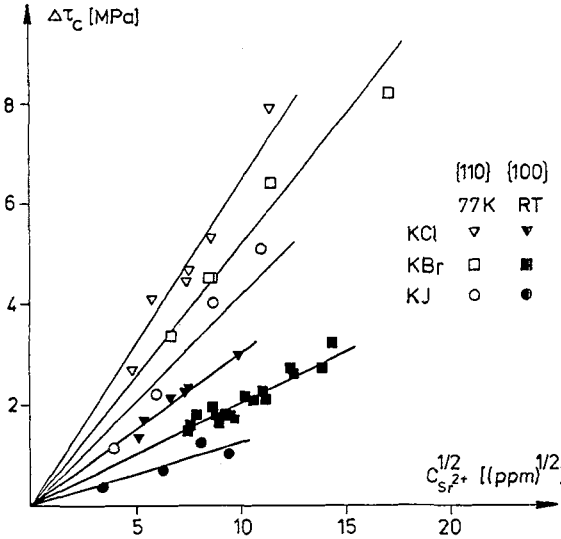
Fig. 14.- Contribution of Sr^{2+} doping to the CRSS as a function of concentration.

According to Ono /28/ the activation energy stress relation can be described for nearly any type of obstacle profile by

$$U(\tau_c) = U_o \left(1 - \left(\frac{\tau_c}{\tau_{co}}\right)^{1/2}\right)^{3/2} \qquad (2)$$

(τ_{co} = CRSS at T=0K). Using an Arrhenius ansatz for the strain rate

$$\dot{a} = a_o \exp\left(-U(\tau_c)/kT\right) \qquad (3)$$

the temperature dependence of the CRSS is given by

$$\left(\frac{\tau_c}{\tau_{co}}\right)^{1/2} = 1 - \left(\frac{T}{T_o}\right)^{2/3} \qquad (4)$$

with

$$T_o = U_o/k \ln(\dot{a}_o/\dot{a}) \qquad (5)$$

The experimental results, figure 15a and b, are in agreement with this theoretical prediction. In figure 15a the "pure" component has not been eliminated. The $\tau_c^{1/2} - T^{2/3}$ curves would however be changed only little by taking into account τ_{cu}. This diagram demonstrates once more the multi-staged decrease of $\tau_c(T)$. Values of the CRSS obtained by extrapolating the temperature dependence of regime II to T = O K are listed in table III. Because of the shortness of regime II these values are

Table III.- Specific hardening in regime II due to short-range interaction between dislocations and IV-dipoles. Quenched crystals are marked by a star.

		LiF	NaCl		KCl	KBr	KJ	AgCl
		Mg^{2+}	Ca^{2+}	Sr^{2+}	Sr^{2+}	Sr^{2+}	Sr^{2+}	Ca^{2+}
$\Delta\tau_{co}/c^{1/2}$ $[10^3\ MPa]$	{100}			$\gtrsim 4.2*$	3.3	3.2	2.2	$\lesssim 0.9$
	{110}	$6 8*^{2),\ 3)}$	$1.6^{1)}$ $1.6*^{4)}$	$1.5*$	1.3	1.2	1.2	
$\Delta\tau_{co}^{\{hkl\}}/c^{1/2}\ \mu^{\{hkl\}}$	{100}			$\gtrsim 0.32*$	0.50	0.62	0.60	$\lesssim 0.13$
	{110}	$0.17*$	0.07 $0.07*$	$0.07*$	0.06	0.07	0.08	

Ref.: [1] /7/, [2] /13/, [3] /29/, [4] /30/

connected with an error of about 20%. The results of table III can be summarized as follows:

- $(\Delta\tau_{co}/c^{1/2})^{\{100\}} > (\Delta\tau_{co}/c^{1/2})^{\{110\}}$, i.e. the specific hardening is greater on {100} than on {110}.

- $(\Delta\tau_{co}/c^{1/2})^{\{110\},\ \{100\}}$ decrease in the series from LiF to AgCl. The decrease is stronger for {100} than for {110} slip.

- $(\Delta\tau_{co}/c^{1/2}\mu)^{\{100\}} \approx 0.5 - 0.62$ (AgCl $\lesssim 0.13$), $(\Delta\tau_{co}/c^{1/2}\mu)^{\{110\}}$ $\approx 0.06 - 0.08$ (LiF $\simeq 0.17$), i.e. the specific hardening is about one order of magnitude greater on {100} than on {110} . The correlation of the specific hardening with the shear modulus alone is again poor.
    Substituting in equation (1) $c_p = \frac{2\sqrt{2}}{3}\ \frac{c}{b^2}$ /31/ and $E_L \simeq \frac{1}{2}\ \mu b^2$ the maximum interaction force is given by

$$f \approx (\Delta\tau_{co}/c^{1/2}\mu)^{2/3}\ \mu b^2 \qquad (6)$$

Values estimated with the help of equation (6) from experiment are pre-
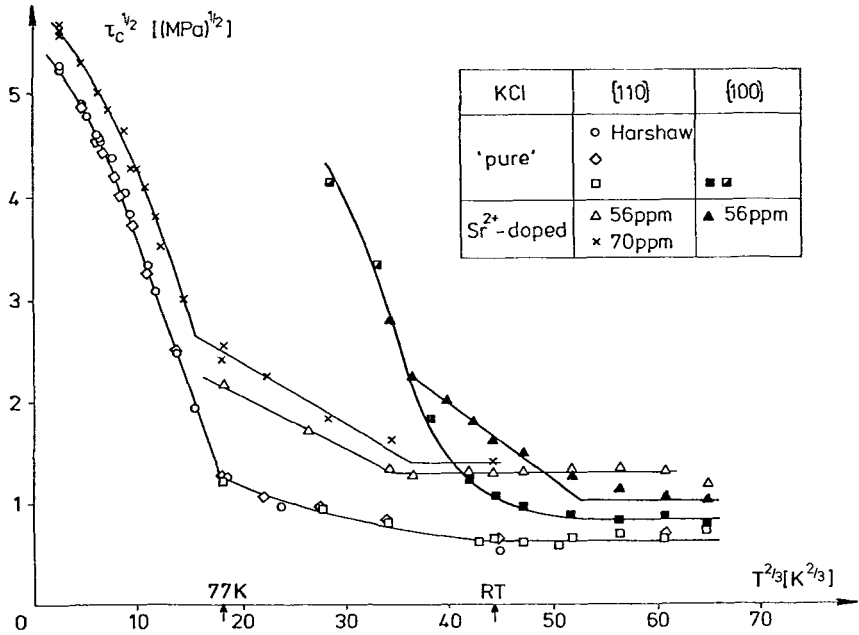
Fig. 15.- a) Temperature dependence of the CRSS of KCl in a $\tau_c^{1/2} - T^{2/3}$ plot, according to Ono.
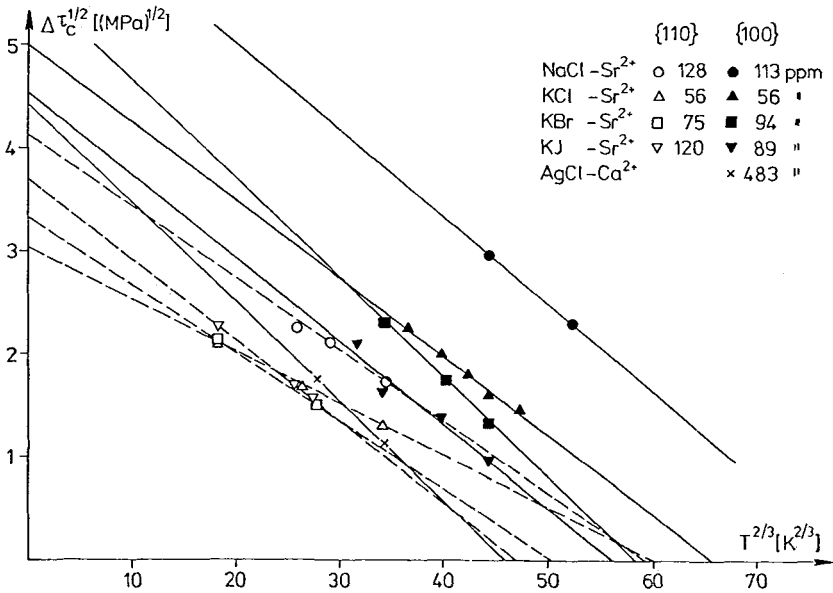
Fig. 15.- b) as (a) for the contribution $\Delta\tau_c^{1/2}$ of Me^{2+} doping.

Table IV.- Comparison of maximum interaction forces between dislocation and IV-dipole. Values in brackets are estimated by taking into account the tetragonal distortion according to the elastic model of Fleischer.

$f \ [10^{-10} \ N]$

| | Experiment | | Theory | | | | | | | | |
| | | | Fleischer | | Gilman | Haasen | | Potstada | | S S H | |
	{110}	{100}	{110}	{100}	{110},{100}	{110}	{100}	{110}	{100}	{110}	{100}
$LiF - Mg^{2+}$	10		5	8	1	1 (6)	5.8 (13.8)				
$NaCl - Sr^{2+}$	6	≳ .10	5	3	0.8	0.8 (5.8)	4.6 (7.6)				
$NaCl - Ca^{2+}$	6		5	3	0.8	0.8 (5.8)	4.6 (7.6)	2 (7)	6.5 (9.5)	3.3	4.7
$KCl - Sr^{2+}$	6	8	6	2	0.8	0.8 (6.8)	4.5 (6.5)				
$KBr - Sr^{2+}$	6	8	6	2	0.7	0.7 (6.7)	4.1 (6.1)				
$KJ - Sr^{2+}$	7	6	6	1	0.6	0.6 (6.6)	3.5 (4.5)				
$AgCl - Ca^{2+}$		≲ 3	4	2	0.5	0.5 (4.5)	2.7 (4.7)				

sented in table IV. In the following model calculations will be compared
with these values regarding the order of magnitude as well as the corre-
lation with ionicity.

A model which has attracted much attention in ionic crystals has
been developed by Fleischer /32/ and is based on the elastic interaction
between a dislocation and the tetragonal distortion around an IV-dipole.
For the closest distance of the dipole to the slip plane (b/2) and for
a defect volume of $2\sqrt{2}\,b^3$ /31/ the maximum interaction force is

$$f \approx \mu b^2 \, \Delta\varepsilon, \tag{7}$$

($\Delta\varepsilon$ = tetragonal distortion).

With $\Delta\varepsilon \approx 0.15$ (see section 4.2.2) values are obtained which are of the
right order of magnitude, but except for LiF the anisotropy comes out
wrong $f^{\{100\}}/f^{\{110\}} \approx \mu^{\{100\}}/\mu^{\{110\}} < 1$. This result is contrary
to the experimental observations.

Gilman /33/ has proposed a short-range interaction which is based
on the increase ΔU of the electrostatic energy during shearing of a
dipole. f is approximately given by

$$f \approx \frac{\Delta U}{b} = 0.3 \frac{e^2}{\varepsilon_o b^2} \, , \tag{8}$$

(e = electron charge).
An extension of this model by Mitchell and Heuer /31/, considering the
displacement field of the dislocation yields values, which are only
30% higher. Gilman's model gives the right correlation of f with the
ionicity but it fails in describing the order of magnitude and does
not take into account the plastic anisotropy.

Haasen /34/ ascribed the extrinsic plastic anisotropy to the elec-
trostatic interaction of edge dislocations with IV-dipoles. This inter-
action is expected to be stronger for a {100} <110> edge dislocation
because its extra half plane ends with equally charged rows of ions,
while for a {110} <110> edge dislocation these rows consist of ions of
alternating charge. Haasen calculates the maximum interaction energy
in two steps. First the extra half plane is neutralized by ions of oppo-
site charge and the interaction of these ions with the foreign ion is
calculated. Secondly changes of this interaction are estimated when the
extra half plane is actually removed and the surrounding lattice is
allowed to relax to a dislocation configuration. f is approximately
derived as

$$f \approx K \frac{e^2}{\varepsilon_o b^2} \tag{9}$$

with

$$K^{\{110\}} = 0.3$$
$$K^{\{100\}} = 1.7$$

Haasen's model neglects the tetragonal distortion of the lattice around the dipole which arises from the attractive electrostatic interaction between divalent ion and vacancy. Taking this into account according to the elastic model of Fleischer, the experimental situation can be explained, i.e. the plastic anisotropy disappears with decreasing ionicity. However, the theory cannot account for the strong difference between KJ and AgCl.

An advanced calculation of the electrostatic interaction energy has been given by Potstada /35/. Using an atomistic model established by Granzer et al. /3/ he calculates a more realistic core configuration and besides the Coulomb interaction he takes into account repulsion and Van der Waals terms as well as polarisation effects around charged point defects. Potstada's calculations are restricted to the maximum interaction energy of isolated Ca^{2+} ions and vacancies with edge dislocations in NaCl. Therefore in the case of dipoles the tetragonal distortion has not been considered. The maximum interaction force estimated agrees quite well with experiment, however.

In previous work of Skrotzki, Steinbrech and Haasen (SSH) /7/ an effective maximum interaction force has been estimated by superposition of the interactions of the two dipole orientations (1 and 2) assumed to be essential:

$$f_{eff} = (\frac{1}{\sqrt{2}} \frac{f_1^2 + f_2^2}{(f_1 + f_2)^{1/2}})^{2/3} \tag{10}$$

f_i consist of the electrostatic interaction calculated by Potstada and an elastic interaction. The agreement with the experimental results is better than a factor two.

For a more accurate analysis complete force distance profiles have to be calculated atomistically. Furthermore it seems to be important to consider different dipole orientations and to superpose their interactions according to a law given by Friedrichs and Haasen /36/. To explain the difference between alkali and silver halides the many-body contribution to the Van der Waals interaction should be taken into account.

4.2.2 Snoek-type interaction (regime III).- The linear concentration dependence as well as the temperature insensitivity of the CRSS are

indicative for a dislocation induced Snoek effect /37,38/. Table V
shows that the contribution to the CRSS due to Snoek-type interaction
is smaller for {100} slip than for {110}. However, $\Delta\tau/c\mu$ is nearly con-
stant for both planes. This means that the Snoek effect is mainly due

Table V.- Specific hardening in regime III due to Snoek-type interactions. Quenched
crystals are marked by a star.

		LiF	NaCl		KCl	KBr	KJ	AgCl
		Mg^{2+}	Ca^{2+}	Sr^{2+}	Sr^{2+}	Sr^{2+}	Sr^{2+}	Ca^{2+}
$\Delta\tau_c/C$ [10^4 MPa]	{100}				0.7	0.6	0.3	
	{110}		$1.9^{1)}$		2.0	1.5	1.0	≥ 0.4
		$2.8*^{2)}$	$2.1*^{3)}$	$1.1*$	$1.8*$	$1.5*$		
$\Delta\tau_c^{\{hkl\}}/C\mu^{\{hkl\}}$	{100}				1.2	1.2	0.8	
	{110}		1.1		1.2	1.0	0.9	≥ 0.4
		0.8*	1.2*	0.6*				

Ref.: ¹⁾ /7/, ²⁾ /13/, ³⁾ /39/.

to an elastic interaction. The short-range electrostatic interaction
is of no importance in decreasing the free enthalpy of the dipoles sur-
rounding a dislocation ("Snoek atmosphere").

The elastic contribution of the Snoek effect to the CRSS has been
estimated by Frank /38/, as

$$\Delta\tau = \alpha\mu\Delta\varepsilon \; c_D \quad , \quad \text{if} \quad \nu_r r_o/v \ll 1 \quad\quad (11)$$

The time r_o/v, required by a dislocation of the velocity v to go through
the radius r_o of the Snoek atmosphere should be small compared with the
time of reorientation of the dipole $1/\nu_r$ (c_D = concentration of IV-di-
poles). With $\alpha \approx 7$ for the stronger interacting edge component reasonable
values for $\Delta\varepsilon$ between 0.1 and 0.2 are obtained. Theoretical calculations
of $\Delta\varepsilon$ are not known, however.

4.2.3. Dissociation and drag of IV-dipoles (regime IV).- According to
the analysis of sections 4.2.1 and 4.2.2 two mechanisms are possible
for the high temperature drop of the CRSS:
- dissociation of the IV-dipoles,
- dragging of the Snoek atomsphere.

The dissociation of dipoles with increasing temperature is quan-
titatively described by the mass-action law

$$\frac{(c-c_D)^2}{c_D} = \frac{1}{12} \ \exp \ (- \Delta g_b/kT) \tag{12}$$

(Δg_b = change of the free entalpy during dissociation). According to equation (11) the Snoek effect decreases by 20%, if $c_D = 0.8 \ c$. This concentration is reached in alkali halides with $c \approx 5 \times 10^{-5}$ and $\Delta g_b \approx$ 0.5 eV /40/ at $T_f/T_m \approx 0.5$ i.e. close to the observed values. The disso- ciation of dipoles cannot however explain the smaller T_f of AgCl, be- cause the binding energy of divalent ions to vacancies in this material is about 0.5 eV /41/, too.

At high temperatures or small strain rates the Snoek atmospheres are able to follow the moving dislocations. According to Frank /38/ in this case equation (11) must be replaced by

$$\Delta \tau_c = \alpha \mu \Delta \varepsilon \ c_D \ f \ (h) \tag{13}$$

with

$$f \ (h) = f(\nu_r r_o/v) \tag{14}$$

For h = 1, f (h) is about 0.8. The condition h = 1 and

$$\nu_r = \nu_{ro} \ \exp \ (-\Delta g_r/kT) \tag{15}$$

$$r_o = \beta \ \Delta \varepsilon \ b \ T_m/T \tag{16}$$

$$v = \dot{a} \ /Nb \tag{17}$$

(Δg_r = free enthalpy of reorientation, N = mobile dislocation density, $\nu_{ro} \approx 5 \times 10^{13} s^{-1}$, $\beta \approx 50$) yields

$$T_f = \frac{\Delta g_r}{h}/\ln \ \frac{\nu_{ro} \beta \ b^2 \Delta \varepsilon \ N \ T_m}{\dot{a} \ T_f} \tag{18}$$

with $\Delta \varepsilon \approx 0.15$, $\dot{a} \approx 10^{-4} s^{-1}$ and $\Delta g_r \approx 0.7$ eV /40/ in alkali halides the mobile dislocation density is about $10^5/cm^2$ at $T_f/T_m \approx 0.5$. Because this value appears reasonable it is assumed that in alkali halides dragging of IV-dipoles contributes to the high temperature drop in CRSS.

4.2.4 Obstacles in "pure" crystals.- The analysis of the hardening due to doping depends on the way of elimination of the "pure" component from the measured CRSS. Therefore it is important to identify the obstacles determining the CRSS of the pure crystals. In the following this will be attempted with the aid of the measured plastic anisotropy.

Table VI.- Plateau stresses of the "pure" crystals.

		NaCl	KCl	KBr	KJ	AgCl
τ_c [MPa]	{100}	2.3	0.7	0.6	0.4	0.5
	{110}	0.65	0.45	0.5	0.45	0.5
$10^4 \ \tau_c^{\{hkl\}}/\mu^{\{hkl\}}$	{100}	2.0	1.2	1.2	1.1	0.8
	{110}	0.4	0.3	0.3	0.4	0.4

Table VI presents the plateau stresses of the "pure" crystals. Striking are the following results:

1) $\tau_c^{\{100\}} \geq \tau_c^{\{110\}}$, i.e. in the plateau range slip on {100} is more difficult than on {110}.

2) $\tau_c^{\{100\}}$ becomes smaller with decreasing ionicity, while $\tau_c^{\{110\}}$ is nearly constant.

3) $(\tau_c/\mu)^{\{100\}} \approx (0.3 - 2) \times 10^{-4}$,

   $(\tau_c/\mu)^{\{110\}} \approx 0.35 \times 10^{-4}$,

i.e. τ_c/μ is about 2 - 5 times larger for cube plane slip.

From 3) it is concluded that the CRSS of the "pure" crystals cannot be determined just by dislocation-dislocation interactions. Considering the intersection of dislocations /42/ or the passing of parallel dislocations the CRSS should be proportional to the shear modulus: $\tau_c \sim \mu b \sqrt{\rho}$ (ρ = dislocation density). The same holds for dipoles of unknown impurities or "eigen"-dipoles of interstitial ions /43/, because in this case the plateau stress should be determined by a Snoek-effect.

Points 1) and 2) suggest the CRSS of the purest investigated crystals to be determined by impurity aggregates. Such aggregates of IV-dipoles or anion complexes -e.g. OH^-, CO_3^{2-}, SO_4^{2-}, O_2^{2-} - are already present in the starting material or may come from the crucible or the atmosphere during crystal growth. Impurity aggregates give rise to short-range electrostatic interaction which should be more important for {100} than for {110} slip. Assuming that all crystals contain about the same concentration of these aggregates the correlation of the plateau stresses with ionicity can be understood. Furthermore aggregates are more difficult to surmount by thermal activation than IV-dipoles yielding only a weakly temperature dependent contribution to the CRSS.

4.3 Interaction_of_dislocations_with_IV-dipole_aggregates.- The tendency

for precipitation of Sr^{2+} ions is stronger in NaCl than in the other investigated crystals as suggested from the dependence of the CRSS on the cooling rate. From the decrease of the dipole concentration during annealing of doped and quenched alkali halides Dryden et al. /24/ conclude that dimers, trimers and higher aggregates of IV-dipoles are formed. In crystals containing such complexes the CRSS is determined by the forces required to cut or pass these aggregates. For a quantitative treatment of this precipitation hardening the knowledge of the particle concentration as well as their size distribution is needed. These informations are not available at present.

From the investigations of Dryden et al. Frank /44/ concludes that after a certain thermal pretreatment of the crystals the IV-dipoles exist in complexes of uniform size consisting of n dipoles. Assuming equilibrium between c_n and the concentration of non-agglomerated dipoles c_D he obtaines for high Me^{2+} concentrations and $n \geq 3$

$$\Delta \tau_c \sim c^{1/2} \tag{19}$$
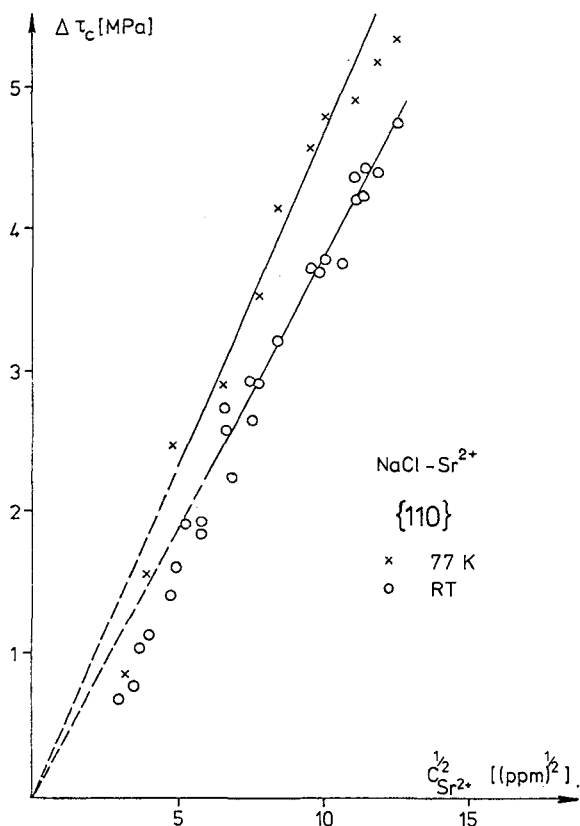

Fig. 16.- Contribution of Sr^{2+} doping to the CRSS of slowly cooled NaCl as a function of the square root of the concentration.

In figure 16 $\Delta\tau_c$ for NaCl - Sr^{2+} is plotted versus the square root of
the total Sr^{2+} content. Assuming that in NaCl the complexes are the do-
mineering obstacles for dislocation motion the "pure" component has
been substracted linearly according to Foreman and Makin /26/. Figure
16 shows that equation (19) holds for concentrations $c_{Sr^{2+}} \gtrsim 30$ ppm.
Furthermore $\Delta\tau_c$ is only weakly temperature dependent. This means, that
aggregates exist of at least three dipoles and that these complexes
are difficult to surmount by thermal activation.

The influence of dipole aggregates on {100} slip cannot be sepa-
rated clearly in NaCl because there exists no distinct range between
regimes I and IV. Quenched crystals show a strong increase of the
CRSS above RT. This increase is probably due to the formation of dipole
aggregates.

For the solubility of impurity atoms in metals the size misfit
is an important parameter. In ionic crystals this misfit is given by

$$\delta = \frac{r_{Me^{2+}} - r_{cation}}{r_{cation}} \tag{20}$$

(r = ionic radius), where

$$\delta = 2\% \text{ between } Na^+ \text{ and } Ca^{2+},$$
$$\delta = 14\% \text{ between } Na^+ \text{ and } Sr^{2+},$$
$$\text{and } \delta = 16\% \text{ between } K^+ \text{ and } Sr^{2+} /45/.$$

These values show that the tendency for aggregation is correctly de-
scribed within the same material (NaCl) but not in comparison with KCl.
Obviously electrostatic interactions play an important role here, too.

References

/1/ Suzuki, T., Kim, H., J. Phys. Soc. Jpn. 39 (1975) 1566

/2/ Suzuki, T., Him, H., J. Phys. Soc. Jpn. 40 (1976) 1703

/3/ Granzer, F., Wagner, G., Eisenblätter, J., Phys. Status Solidi 30 (1968) 587

/4/ Frank, W., Phys. Status Solidi 29 (1968) 391

/5/ Suszynska, M., Bull. Acad. Pol. Sci. Ser. Sci. Tech. 25 (1977) 315

/6/ Grau, P., Fröhlich, F., Phys. Status Solidi A 55 (1979) 479

/7/ Skrotzki, W., Steinbrech, R., Haasen, P., Mater. Sci. Eng. 32 (1978) 551

/8/ Aßmus, W., Pappert, G., Granzer, F., J. Cryst. Growth. 41 (1977) 172

/9/ Skrotzki, W., Ph. D. Thesis, Göttingen (1980)

/10/ Bhagavan Raju, I.V.K., Strunk, H., Phys. Status Solidi A 53 (1979) 211

/11/ Suzuki, T., Skrotzki, W., Haasen, P., Phys. Status Solidi A to be published

/12/ Franzbecker, W., Diploma Thesis, Göttingen (1969)

/13/ Johnston, W.G., J. Appl. Phys. 33 (1962) 2050

/14/ Gilman, J.J., Acta Metall. 7 (1959) 608

/15/ Buerger, M.J., Am. Mineral. 15 (1930) 226, 16 (1931) 237

/16/ Bücher, M., Ph. D. Thesis, Frankfurt (1977)

/17/ Granzer, F., "DGPh Intern", Sonderausgabe zum Münchner Symposium, (1979), private communication

/18/ Huntington, H.B., Dickey, J.E., Thomson, R., Phys. Rev. 100 (1955) 1117

/19/ Puls, M.P., So, C.B., Phys. Status Solidi B 98 (1980) 87

/20/ Hoagland, R.G., Hirth, J.P., Gehlen, P.C., Philos. Mag. 34 (1976) 413

/21/ Woo, C.H., Puls, M.P., J. Phys. C 9 (1976) 127

/22/ Puls, M.P., AECL report 6929 (1980)

/23/ Kataoka, T., Uematsu, T., Yamada, T., Jpn. J. Appl. Phys. 17 (1978) 217

/24/ Dryden, J.S., Morimoto, S., Cook, J.S., Philos. Mag. 12 (1965) 379

/25/ Labusch, R., Acta Metall. 20 (1972) 917

/26/ Foreman, A.J.E., Makin, M.J., Philos. Mag. 14 (1966) 911

/27/ Frank, W., Mater. Sci. Eng. 6 (1970) 132

/28/ Ono, K., J. Appl. Phys. 39 (1968) 1803

/29/ Guiu, F., Langdon, T.G., Philos. Mag. <u>30</u> (1974) 145

/30/ Suzuki, T., unpublished

/31/ Mitchell, T.E., Heuer, A.H., Mater. Sci. Eng. <u>28</u> (1977) 81

/32/ Fleischer, R., Acta Metall. <u>10</u> (1962) 835

/33/ Gilman, J.J., J. Appl. Phys. <u>45</u> (1974) 508

/34/ Haasen, P., in: Dislocations et Processes de Transport, J.
     Physique Colloq. <u>9</u> (1973) C9- 205

/35/ Potstada, H.H., Diploma thesis, Frankfurt (1975)

/36/ Friedrichs, J., Haasen, P., Philos. Mag. <u>31</u> (1975) 863

/37/ Schoeck, G., Seeger, A., Acta Metall. <u>7</u> (1959) 469

/38/ Frank, W., Z. Naturforsch. <u>22a</u> (1967) 377

/39/ Hesse, J., Phys. Status Solidi A <u>21</u>, (1967) 495

/40/ Barr, L.W., Lidiard, A.B., in Physical Chemistry, Vol. <u>X</u>
     (Acad. Press N.Y./London) 1970

/41/ Abbink, H.C., Martin, D.S., J. Phys. Chem. Solids <u>27</u>
     (1966) 205

/42/ Frank, W., Mater. Sci. Eng. <u>6</u> (1970) 121

/43/ Frank, W., Phys. Status Solidi <u>29</u> (1968) 391

/44/ Frank, W., Phys. Status. Solidi <u>29</u> (1968) 767

/45/ Shannon, R.D., Prewitt, C.T., Acta Crystallogr. Sect. B <u>25</u>
     (1969) 925